Vol. 38, No. 3 (2016) 425-434

Tribology in Industry

www.tribology.fink.rs

RESEARCH

Analysis of Tribological Behaviour of Functionally Graded LM13 Aluminium/TiS_2 Composite Using Design of Experiments

N. Radhika[a]

[a] *Department of Mechanical Engineering, Amrita School of Engineering, Coimbatore, Amrita Vishwa Vidyapeetham, Amrita University, Tamilnadu, India.*

Keywords:

Aluminium
Centrifugal casting
Dry sliding wear
Analysis of variance
Scanning electron microscope

Corresponding author:

N. Radhika
Department of Mechanical Engineering,
Amrita School of Engineering, Coimbatore,
Amrita Vishwa Vidyapeetham,
Amrita University,
India.
E-mail: n_radhika1@cb.amrita.edu

A B S T R A C T

Functionally graded LM13 aluminium/10wt% TiS_2 composite was fabricated by centrifugal casting method and hollow cylindrical part has the dimension of 150x150x20 mm was obtained. The microstructural evaluation and vicker's micro-hardness test was carried out on the surfaces at the distance of 1, 6, 12 and 18 mm from the outer surface of functionally graded composites. The microstructural investigation reveals that the TiS_2 reinforcement particles concentrated more on the outer periphery and less at the inner periphery of the composite. The hardness of the composite surface increases at the particle rich region of outer periphery and decreases towards inner region. The dry sliding wear experiments were conducted on the composite specimens as per plan of Taguchi's L_{16} orthogonal array design. The parameters considered were load, sliding velocity, sliding distance and distance from outer periphery of the composite, varied for four levels. Signal- to- Noise ratio and Analysis of Variance were carried out and the significance test revealed that distance from outer periphery had major impact (43.11 %) followed by sliding distance (31.19 %), load (16.59 %), and sliding velocity (7.33 %). Adequacy of model was predicted through regression equation and the error was found to be less than 8 %. The scanning electron microscope analysis carried out for the worn-out surfaces showed maximum wear resistance of the functionally graded composite at outer periphery.

1. INTRODUCTION

Aluminium is an attractive metal known by its less weight, high thermal and electrical conductivity. Aluminium Matrix Composites (AMCs) are developed for greater strength, high stiffness, high abrasive and wear resistance [1]. AMCs play major role in different industries such as automotive, aerospace and defence. These composites utilised best alternate to monolithic materials [2].The aluminium matrix can be strengthened by the hard reinforcement particles like Silicon Carbide (SiC), Alumina (Al_2O_3) and Boron Carbide (B_4C) [3]. The stir

casting process found to be the most economic way to distribute the particles in uniform and produces defect-free casting [4]. B_4C particle reinforced AMCs are fabricated by this method and the result shows that increase in B_4C content increases the hardness and tensile properties [5]. Carbon nanotube reinforced aluminium matrix also exhibits higher tensile strength compared to pure aluminium.

An advanced composite which composed of dual materials that have gradual variation in composition and structure gives multiple properties throughout the material known as Functionally Graded Material (FGM).Several fabrication methods are available, among them centrifugal casting method found to be easy and less expensive way to produce FGM [6]. Hardness test was carried on 356 and 2124 aluminium alloy reinforced with SiC particles prepared by horizontal centrifugal casting. The result shows that Al356 SiC-functionally graded composite exhibits higher hardness value of 155 BHN on outer periphery of the composite compared to Al2124 SiC- functionally graded composite [7]. Abrasive wear behaviour of Al_2O_3 reinforced aluminium composite and unreinforced aluminium alloy is investigated under constant load and at different sliding distances. The result reveals that incorporation of Al_2O_3 particles shows greater abrasive resistance than the aluminium alloy and the wear rate is found increased with increase in sliding distance [8]. FGM tubes are manufactured from plaster matrix through centrifugal method and the result reveals that the higher density particles are located at outer tube due to centrifugal force [9]. The tribological behaviour of aluminium reinforced flyash particles is investigated and the result explores that the aluminium composite has higher wear resistance compared to unreinforced material [10].

Design of Experiments (DOE) is an optimization tool to find the various factors and facilitating the design model. It becomes the major technique to minimize the experimental error and allow to know which parameter has significant impact in the experimental analysis [11,12]. The wear prediction model is developed using Taguchi's orthogonal design method for aluminium/aluminium diboride (AlB_2) composite with different wt% and wear testing parameters selected are sliding velocity, load, sliding distance and reinforcement ratio. The result reveals that the load influences higher wear rate followed by reinforcement ratio and sliding velocity [13]. The dry sliding wear behaviour of epoxy resin reinforced flyash particles is investigated and results are compared under the Taguchi's orthogonal array model. The parameter applied load found to be the most influence on increase in wear rate [14]. Researchers found that DOE method greatly helps the engineers to improve the production rate at low level variability [15].

From the above literature survey, the studies of functionally graded titanium disulfide aluminium composites are not explored extensively. Thus the present work focused on tribological behaviour of functionally graded aluminium LM13/titanium disulphide (TiS_2) composite produced through centrifugal casting route.

2. SELECTION OF CONSTITUENTS

The LM13 aluminium alloy is chosen as the matrix material, as it has the application particularly in the engine parts at elevated temperature and also exhibits good bearing properties. TiS_2 is selected as the reinforcement particles due to its high wear resistance and hardness properties. TiS_2 reinforcement particles with an average size of 12 μm and the content of 10wt% are taken. The density of aluminium alloy and TiS_2 particles are 2.70 g/cm^3 and 3.22 g/cm^3 respectively.

3. FABRICATION PROCESS

Aluminium LM13 ingots are taken in the graphite crucible and loaded inside the electric furnace (Fig. 1) for melting. Simultaneously the TiS_2 reinforcement particles are placed in another crucible and preheated (350 ^oC) inside the furnace. To avoid the defects during casting, argon gas is supplied inside the heating chamber. When the ingot melts and become molten state, the preheated TiS_2 reinforcement particles are gradually added through the hopper provided at top of the furnace. The stirrer setup with gear reduction system is placed above the furnace through which the stirring is carried out in the molten metal containing reinforcement particles at 200 rpm

for 5 minutes. This stirring effect produces vortex action which sucks the particles inside the molten metal and helps to distribute the particles uniformly in molten metal. In order to produce the FGM, horizontal centrifugal casting method is used (Fig. 2). To maintain the temperature difference between the molten metal and inner surface of centrifugal die, the die surface is preheated for 350^{0}C and allowed to rotate at 1200 rpm. The stirred molten metal is taken out from the furnace and poured through hopper of centrifugal die.

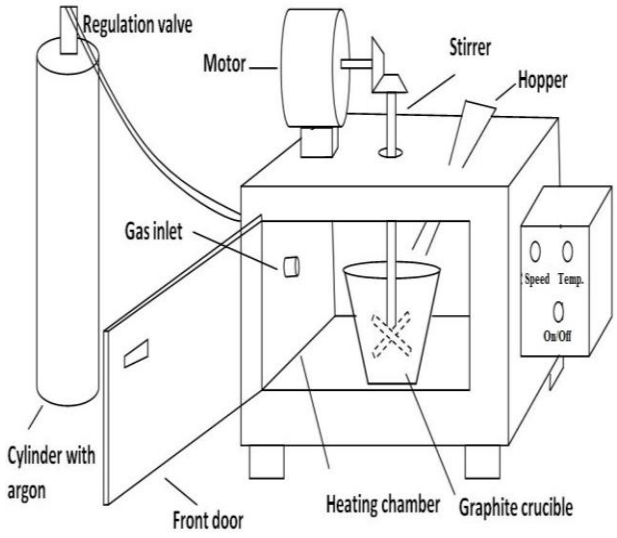

Fig. 1. Electric resistance furnace with stirrer set up.

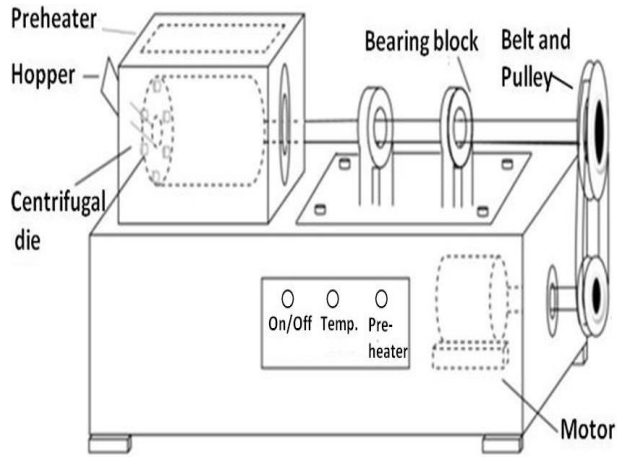

Fig. 2. Centrifugal casting setup.

The centrifugal action takes place in the molten metal containing reinforcement particles. This centrifugal force is calculated by using the relation $F_c = m\omega^2 r$ and the gravitational force is given by mg. The ratio of the centrifugal force to the gravitational force gives the gravitational co-efficient (G) and is given by $G = \omega^2 r/g$. The rotation continues till the completion of solidification of molten metal. After the solidification, the cast hollow cylindrical part (150 x 150 x 20 mm) is removed from the die.

4. MICROSTRUCTURAL INVESTIGATION

The surfaces which are at the distance of 1, 6, 12 and 18 mm from outer periphery of the functionally graded composite are taken for microstructural examination. To attain crystal like surface, the specimen is well polished by the linisher polisher followed by emery sheets of grades 1/0 and 2/0. Then the specimen of composite is polished on disc polisher in the presence of diluted alumina (Al_2O_3). Prior to observation in Zeiss Axiovert 25 CA Inverted Metallurgical Microscope, etching is done by using keller's reagent to highlight the microstructure present in the specimen and also to increase the specimen surface quality.

5. HARDNESS EVALUATION

The composite specimen surfaces are polished using the emery sheets 1/0 and 2/0 to attain smooth surface finish and the hardness test is conducted at the distance of 1, 6, 12 and 18 mm from outer periphery. The specimen is fitted into the base plate of the Vickers hardness tester and positioned by the movable mechanical jaws. The diamond indenter is utilised for making the indentation on the surface of specimen. The indenter dropped on the surface of the specimen under the load of 100 gf for 10 seconds. Then the indenter released mechanically from the surface and the impression diagonal lengths are measured to obtain the hardness value of the surface. The hardness test is repeated for 5 times in different places on the surface of the specimen and the average is taken for evaluation.

6. DESIGN OF EXPERIMENTS

To carry out the DOE, four parameters chosen are load, sliding velocity, sliding distance and distances (1, 6, 12 and 18 mm) from outer periphery of the functionally graded composite for which the response taken is dry sliding wear rate. Based on the parameter factors and levels, Taguchi's L_{16} orthogonal array design is taken for optimizing the conditions.

7. DRY SLIDING WEAR TEST

To analyse the tribological properties of functionally graded composite, pin-on-disc tribometer is used (Fig. 3). The dry sliding wear tests are conducted as per ASTM G99-04 standard on the specimen [17].

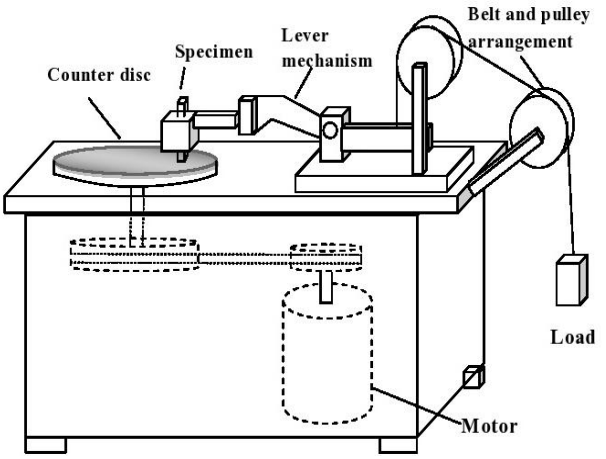

Fig. 3. Pin-on-disc dry sliding wear tester.

The specimen pin is properly cleaned with acetone and weighed in a precision weighing balance with an accuracy of 0.1 mg. The composite specimen is fixed in the holder which is perpendicular to the rotating counter disc made up of hardened steel (EN-32) and facilitates to make the specimen contact against the counter surface. The specimen holder attached with lever arm has weight adding pan and allowed to add weight by the required load condition. This induces the specimen to press against the rotating disc and the test is conducted in the sequential order as per the plan of L_{16} orthogonal array model. After the completion of the experiment, specimen is removed from the holder and it is weighed again for predicting the mass loss and finally wear rate is calculated using Eqn. (1).

$$W = \frac{\mathrm{M}}{\rho \mathrm{D}} \tag{1}$$

where '*W*' is wear rate (mm^3/m), 'M' is mass loss (g), 'ρ' is density (g/mm^3) and 'D' is the sliding distance (m).

8. RESULT AND DISCUSSIONS

The experimental results of microstructural evaluation, hardness test, and dry sliding wear test are briefly discussed in following subsection.

8.1 Microstructural investigation

The composite surface at the distance of 1 mm (Fig. 4a) has the presence of more reinforcement particles; this is due to the centrifugal force created by rotating die which moves higher density reinforcement particle towards the outer periphery. At the surface of 6 mm, (Fig. 4b) fewer reinforcement particles is found and comparatively less count of particles is observed at 12 mm distance from outer periphery (Fig. 4c).

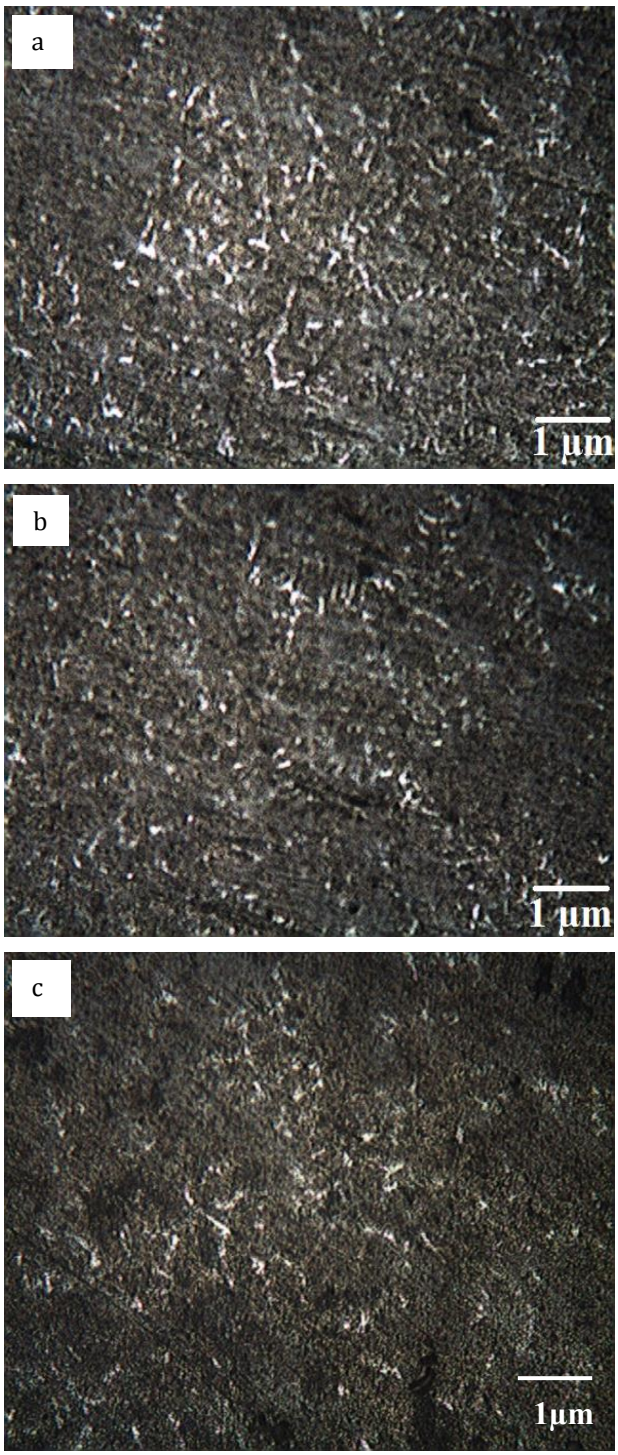

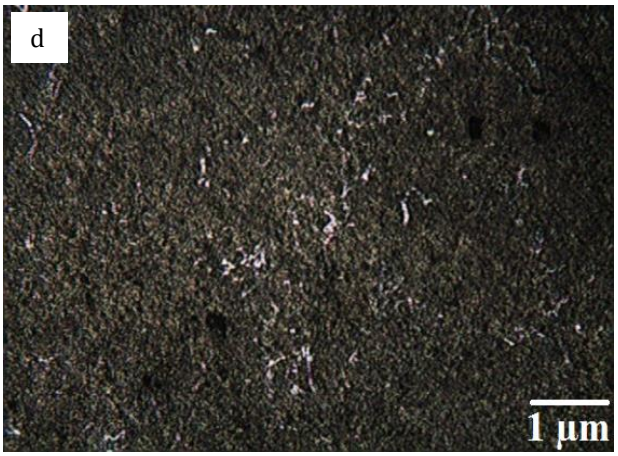

Fig. 4. Microstructure of the FGM at various distances from outer periphery a) 1 mm, b) 6 mm c) 12 mm and d) 18 mm.

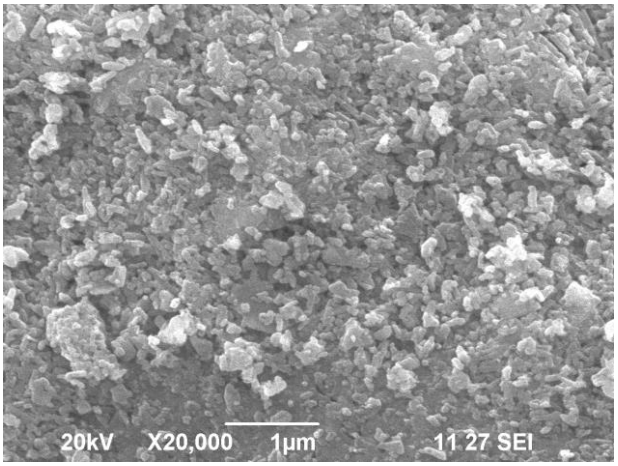

Fig. 5. SEM image of TiS_2 particles.

The surface at the distance of 18 mm (Fig. 4d) has very less particles and this is due to less dense gas bubbles moves from outer to inner periphery in reverse cycle during the casting process which takes few reinforcement particles along with it and settles at the inner periphery. The TiS_2 particles used for functionally graded composites are examined through Scanning Electron Microscope (SEM) analysis and shown in Fig. 5.

8.2 Hardness evaluation

The hardness test result reveals that the composite surface at the distance of 1 mm has higher hardness value of 120 HV (Fig. 6) compared to other surfaces and this region leads to resist indentation. By the evidence of microstructural results, it is observed that concentration of TiS_2 particles are more at the outer periphery (Fig. 4a) of the composite and this segregation of particles in the composite decides the hardness value.

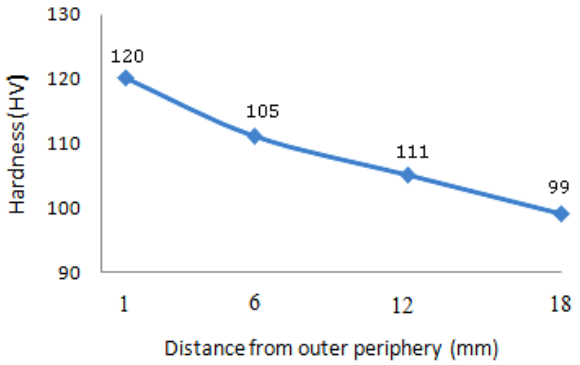

Fig. 6. Hardness of the composite at different distances.

When the reinforcement particles decreases towards the inner periphery it tends to decrease the hardness of the composite specimen.

8.3 Wear behaviour

The parameter levels selected for the wear test is shown in Table 1.

Table 1. Parameters and levels.

Levels	Load (N)	Sliding Distance (m)	Sliding Velocity (m/s)	Dist. from Outer periphery (mm)
1	15	500	1	1
2	25	1000	2	6
3	35	1500	3	12
4	45	2000	4	18

The wear experimental results obtained from the L_{16} orthogonal array design is shown in Table 2.

Tables 2. Experimental wear results.

S. No	Load (N)	Sliding Distance (m)	Sliding Velocity (m/s)	Dist. from Outer Periphery (mm)	Wear Rate (mm^3/m)	S/N Ratio (dB)
1	15	500	1	1	0.0015	56.478
2	15	1000	2	6	0.0020	53.979
3	15	1500	3	12	0.0023	52.765
4	15	2000	4	18	0.0025	52.041
5	25	500	2	12	0.0030	50.458
6	25	1000	1	18	0.0035	49.119
7	25	1500	4	1	0.0020	53.979
8	25	2000	3	6	0.0015	56.478
9	35	500	3	18	0.0039	48.179
10	35	1000	4	12	0.0036	48.874
11	35	1500	1	6	0.0020	53.979
12	35	2000	2	1	0.0016	55.918
13	45	500	4	6	0.0030	50.458
14	45	1000	3	1	0.0032	49.897
15	45	1500	2	18	0.0038	48.404
16	45	2000	1	12	0.0018	54.895

8.4 Signal-to-Noise ratio analysis

The S/N ratio values obtained are analysed through the Minitab statistical software and the response table is obtained (Table 3) for the wear characteristic "smaller-the-better". The response table gives the influencing order of the parameters on the dry sliding wear rate. The high influencing parameter is determined through its delta value. The maximum and minimum value difference of the S/N ratios gives the delta value. The parameter with the highest delta value denotes that it has major impact on the wear rate.

Table 3. Response table for S/N ratios.

Level	Load (N)	Sliding distance (m)	Sliding velocity (m/s)	Distance from outer periphery (mm)
1	53.82	51.39	53.62	54.07
2	52.51	50.47	52.19	53.72
3	51.74	52.28	51.83	51.75
4	50.91	54.83	51.34	49.44
Delta	2.9	4.37	2.28	4.63
Rank	3	2	4	1

From the Table 3, it is observed that distance from outer periphery has more impact on wear followed by sliding distance, load and sliding velocity.

8.5 Influence of Parameters on wear behaviour

The S/N ratio and mean plots obtained are shown in [Fig. 7 and Fig. 8]. From Fig. 7, the optimum values of S/N ratios obtained to achieve minimum wear rate are load of 15 N, sliding distance of 2000 m, sliding velocity of 1 m/s and distance from outer periphery of 1 mm. The mean plot shows the wear rate for each parameter levels.

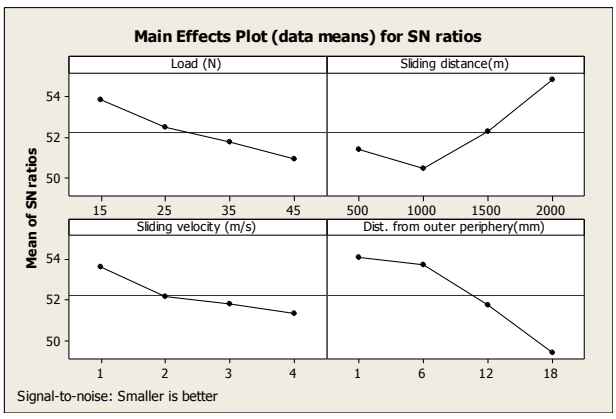

Fig. 7. Main effects plot for S/N ratio - Wear rate.

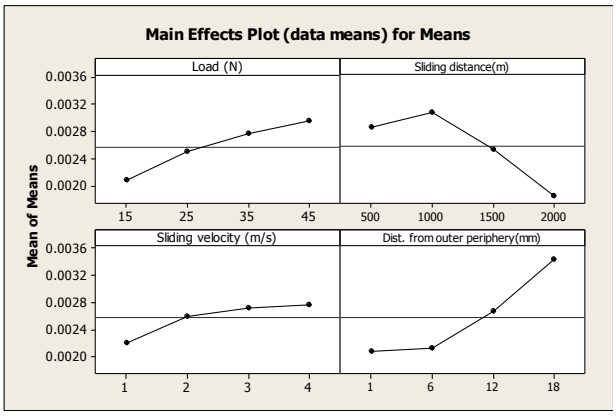

Fig. 8. Main effect plot for mean - Wear rate.

8.6 Effect of load on dry sliding wear rate

Variation of wear rate with variation of applied load is shown in Fig. 8. It is observed from the figure that wear rate of the composite increases with increase in applied load, because as applied load increases, the friction between the contact surface of the composite material and the rotating disc increases. Also due to increase of interfacial temperature, the material becomes ductile which leads to decrease the strength of composite. The contact pressure at the interface of the composite and counterface is higher with increase of load from 15 N to 25 N, as a result sudden increase in wear loss of composite takes place. At the load of 25 N wear loss increases continuously due to the adhesive action and once it reaches to 45 N severe wear takes place and similar phenomenon is observed [16].

8.7 Effect of distance from outer periphery of FGM on dry sliding wear rate

Initially, a slight increase in wear rate of the composite is observed from the distances of 1 mm to 6 mm as shown in Fig. 8. This is due to the presence of higher concentration of reinforcement particles in the region which highly bears the sliding action and avoids the greater removal of surface material. Further, increase in distance from 6mm to 18 mm, abrupt increase in wear rate of the composite is observed. This is due to lesser concentration of reinforcement particles present in composite which makes the surfaces softer leads to increase the wear rate and the same trend is observed (17). Hence wear rate of the composite decreases with increase in concentration of TiS_2 reinforcement particles with aluminium matrix.

8.8 Effect of sliding distance on dry sliding wear rate

It is observed that there is significant increase in wear rate with increase in sliding distance from 500 m to 1000 m (Fig. 8). This is because initially the asperities are harder and sharper, so there is a higher amount of stress acts on the asperity contact. The higher amount of stress leads to plastically deform the asperities and some of the asperity gets fractured. With further increase in sliding distance from 1000 m to 2000 m, wear rate decreases effectively because of the generation of temperature rise to some critical value at which surface gets oxidized and this oxidized surface gets fragmented. The fragmented oxide particle acts as a lubricating agent and effectively reduces the wear rate of composites.

8.9 Effect of sliding velocity on dry sliding wear rate

From Fig. 8 it is observed that wear rate increases suddenly from the sliding velocity of 1 m/s to 2 m/s. This is because, increase of sliding velocity leads to rise in temperature, so reinforcement particles are detached from the matrix due to creation of higher rubbing action and hence wear rate of the composite increases. With further increase in sliding velocity from 2 m/s to 4 m/s, a delay of sudden increase in wear rate is observed due to lesser contact time between specimen surface and counter disc. Also, softening of the composite surface occurs as a result of rise in interfacial temperature. At this stage, material transfer takes place and mechanically mixed layer thus formed become unstable. Hence wear rate increases slightly at the higher velocities.

8.10 Analysis of Variance

The performance of various parameters and its contributions are measured through ANOVA. The obtained value for R^2 (98.76) and R^2 adj (93.76) are found closer. The percentage contributions of each parameter are displayed in the last column in Table 4. The distance from outer periphery has major contribution (43.11 %) followed by sliding distance (31.19 %), load (16.59 %) and sliding velocity (7.33 %) of the FGM.

Table 4. Analysis of Variance for wear rate

Source	DF	Seq SS	Adj SS	Adj MS	F	P	Pct (%)
Load (N)	3	1.7E-06	1.7E-06	6E-07	12.9	0.032	16.6
Sliding distance (m)	3	3.4E-06	3.4E-06	1.1E-06	25.3	0.012	31.2
Sliding velocity (m/s)	3	8E-07	8E-07	3E-07	6.04	0.087	7.33
Outer distance (mm)	3	4.7E-06	4.7E-06	1.6E-06	35.1	0.008	43.1
Error	3	1E-07	1E-07	0			0.9
Total	15	1.1E-05					

9. Regression model

Minitab software is used to develop the linear regression model which tends to give the relation between the experimental and predicted results of dry sliding wear. The developed linear equation is formed by the significant terms of ANOVA. The linear regression equation for wear rate (mm^3/m) is given in Eqn. 2.

$$\text{Wear rate} = 0.00137 + 0.000029\ L - 0.000001\ S.D + 0.000185\ S.V + 0.000082\ D \quad (2)$$

where: L is the load (N), S.D is the sliding distance (m), S.V is the Sliding velocity (m/s), and D is the distance from outer periphery (mm).

The positive sign denotes increasing trend of wear rate and negative sign indicates that the wear rate decreases as performance value increases. The confirmation experimental model is developed for the required levels and wear test is performed on the preferred parameters (Table 5). Regression wear rate is calculated through the Eq. (2) by substituting the selected new set of values.

Table 5. Results of Confirmation experimental model and regression model for wear behaviour.

S. no	Load (N)	Sliding distance (m)	Sliding velocity (m/s)	Distance from outer periphery (mm)	Experimental wear rate (mm^3/m)	Regression wear rate (mm^3/m)	Error %
1	20	600	1.5	4	0.0024	0.0016	8
2	30	1200	2.5	9	0.0027	0.0022	5
3	40	1600	3.5	15	0.0032	0.0028	4

The confirmation experimental result is compared with regression relation and the minimum error (8 %) is found from analysis which indicates that constructed model has greater efficiency.

10. SCANNING ELECTRON MICROSCOPY ANALYSIS

The Scanning Electron Microscopy (SEM) analysis is done on the worn surfaces of the functionally graded composite to observe the wear mechanism during the dry sliding wear test. The surface at 1 mm (Fig. 9a) from outer periphery has less scratch and less material removal rate is observed due to more reinforcement particles present in that region. As the surface distance increases towards inner periphery, there is a change of wear mechanism from mild to severe wear. At the distance of 6 mm (Fig. 9b) and 12 mm (Fig. 9c), deep grooves with severe delamination are observed and are due to the existence of comparatively lesser amount of reinforcement particles. The SEM analysis at the distance 18 mm (Fig. 9d) has more scratch and deep ploughing action as the contact exists between matrix and counter disc during wearing process.

The surface becomes soft due to the very negligible amount of reinforcement particles present in the inner periphery and forms particle depleted area which leads to increase the material removal rate and similar result is observed in another study [18]. Thus it can be concluded that, the particle rich region of 1 mm with higher hardness and wear resistance makes the composite suitable for the applications such as in cylinder liners and brake drum.

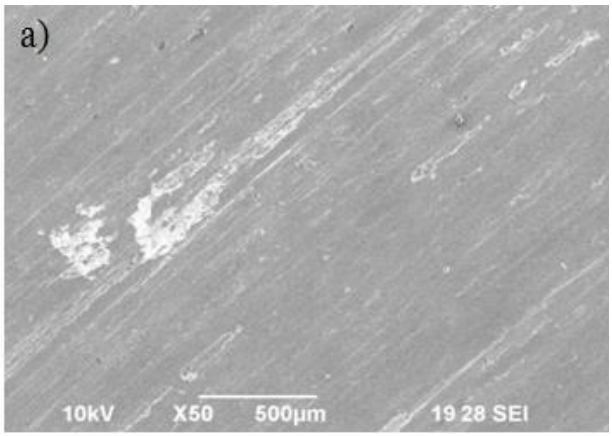

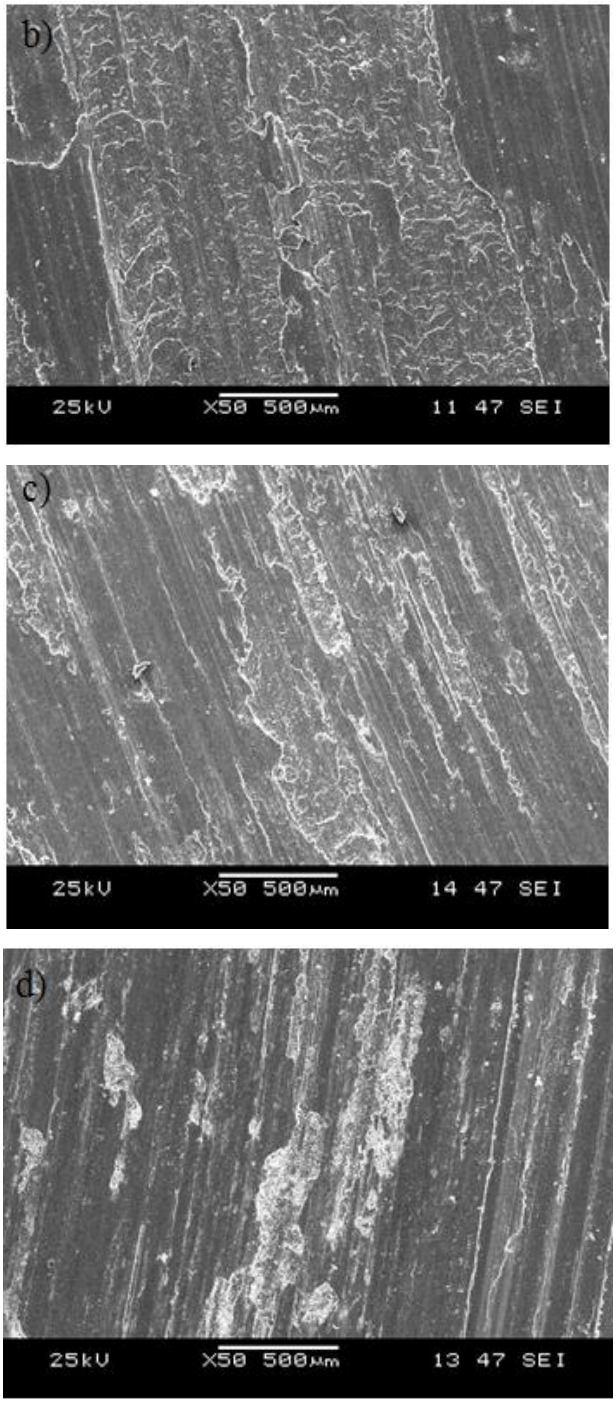

Fig. 9. SEM analysis of worn out surfaces: a) D=1 mm, L=15 N, S.D=500 m, S.V=1 m/s; b) D=6 mm, L=15 N, S.D=1000 m, S.V=2 m/s; c) D=12 mm, L=15 N, S.D=1500 m, S.V=3 m/s and d) D=18 mm, L=15 N, S.D=2000 m, S.V=4 m/s.

The worn-out surface at optimum values (Load = 15 N, Sliding velocity = 1 m/s, Sliding distance= 2000 m, Distance from outer periphery = 1mm) shown in Fig. 10 reveals less wear rate which attributes the composite surface with rich reinforcement region that tends to resist the impact of wear.

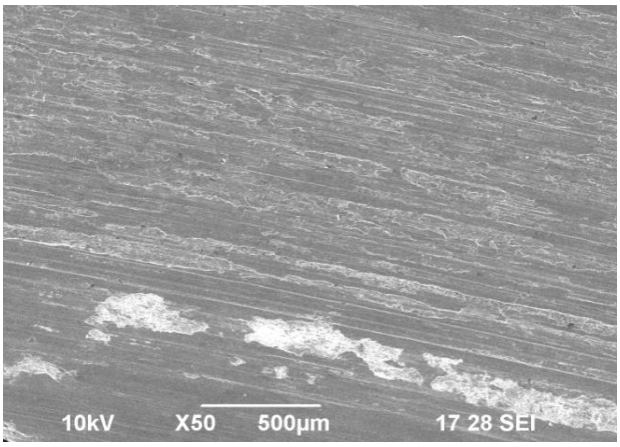

Fig. 10. SEM examination of the worn-out surface at optimum condition.

11. CONCLUSION

The functionally graded aluminium/TiS_2 composite is successfully fabricated by the centrifugal casting process. The microstructural analysis shows that, at the distance 1mm from the outer periphery has particle rich region than the distance of 6 mm, 12 mm and 18 mm. The micro-hardness result shows composite surface at the distance 1 mm has higher hardness value of 120 HV. Taguchi's L_{16} orthogonal model is developed for conducting the dry sliding wear test and the adequacy model from analysis of variance shows that the distance from the outer periphery has the major impact on the wear behaviour of the composite. The optimised conditions obtained are load of 15 N, Sliding velocity of 1 m/s, Sliding distance of 2000 m, Distance from outer periphery of 1mm. The worn out surface of the particle rich region reveals lesser wear rate which is observed by SEM. The results obtained from this functionally graded material can be used efficiently for the applications where tribological performance is a major requirement.

REFERENCES

[1] T.P.D. Rajan and B.C. Pai, 'Formation of solidification microstructures in centrifugal cast functionally graded aluminium composites', Trans*. Ind. Inst. Met*., vol. 62, pp. 383-389, 2009.

[2] T.P.D. Rajan, R.M. Pillai and B.C. Pai, 'Characterization of centrifugal cast functionally graded aluminum-silicon carbide metal matrix composites', *Mater. Charact.*, vol. 61, pp. 923-928, 2010.

[3] Z. Humberto Melgarejo, O.M. Suarez and K. Sridharan, 'Wear resistance of a functionally-graded aluminum matrix composite', *Scr. Mater*., vol. 55, pp. 95-98, 2006.

[4] M.R. Derakshen, H. Sina and H. Nazemi, 'The comparison of microstructure and hardness of Al-B and Al-Mg-B composites', Majilesi *J. Mech. Eng.*, vol. 4, no. 4, pp. 27–31, 2011.

[5] S. Kumar, V.S. Sarma and B.S. Murty, 'Functionally graded Al alloy matrix in-situ composites', *Metall. Mater*. *Trans*., vol. 41A, pp. 242-254, 2010.

[6] Z.H. Melgarejo, O.M. Suarez and K. Sridharan, 'Microstructure and properties of functionally graded Al–Mg–B composites fabricated by centrifugal casting', *Compos. Part A*., vol. 39, pp. 1150-1158, 2008.

[7] A.C. Vieira, P.D. Sequeira, J.R. Gomes and L.A. Rocha, 'Dry sliding wear of Al alloy/SiC_p functionally graded composites: Influence of processing conditions', *Wear*, vol. 267, pp. 585-592, 2009.

[8] A. Jayakumar and M. Rangaraj, 'Property analysis of aluminium (LM-25) metal matrix composite', *Int. J. Emerg. Technol. Adv. Engg.*, vol. 4, no. 2, pp. 495-501, 2014.

[9] O. Savas, R. Kayikci, F. Ficici and S. Koksal, 'Production of functionally graded AlB_2/Al-4%Mg composite by centrifugal casting', *Period. Engg. Nat. Sci*., vol. 1, no. 2, pp. 38-43, 2013.

[10] P. Sharma, G. Chauhan and N. Sharma, 'Production of AMC by stir casting- an overview', *Int. J. Contemp*. *Practic*., vol. 2, no. 1, pp. 23-46, 2013.

[11] C.Y. Lin, C. Bathias, H.B. Mc Shane and R.D. Rawlings, 'Production of silicon carbide Al 2124 alloy functionally graded materials by mechanical powder metallurgy technique', *Powder. Metall*., vol. 42, pp. 29-33, 1999.

[12] N. Radhika, A. Vaishnavi and G.K. Chandran, 'Optimisation of dry sliding wear process parameters for aluminium hybrid metal matrix composites', *Tribology in Industry*, vol. 36, no. 2, pp. 188-194, 2014.

[13] E. Askari, M. Mehrali, I.H.S.C. Metselaar, N.A. Kadri and Md.M. Rahman, 'Fabrication and mechanical properties of Al_2O_3/SiC/ZrO_2 functionally graded material by electrophoretic deposition', *J. Mech. Behav*. *Biomed. Mater*., vol. 12, pp. 144-150, 2012.

[14] M. Nagaral Vauradi and M.K. Ravishankar, 'Mechanical behaviour of aluminium 6061 alloy reinforced with Al_2O_3& graphite particulate

hybrid metal matrix composites', *Int. J. Res. Engg. Technol.,* vol. 1, no. 2, pp. 193-198, 2013.

[15] M. Kok and K. Ozdin, 'Wear resistance of aluminium alloy and its composites reinforced by Al_2O_3 particles', *J. Mater. Process. Technol.,* vol. 183, no. 2, pp. 301-309, 2007.

[16] L.V. Priyanka Muddamsetty and N. Radhika, 'Effect of heat treatment on the wear behavior of functionally graded LM13/B_4C composite'. *Tribology in Industry*, vol. 38, no. 1, pp. 108-114, 2016.

[17] T.P.D. Rajan, E. Jayakumar and B.C. Pai, 'Developments in solidification processing of functionally graded aluminium alloys and composites by centrifugal casting technique', *Trans. Indian. Inst. Met*., vol. 65, no. 6, pp. 531-537, 2012.

[18] N. Radhika and R. Raghu, 'Mechanical and tribological properties of functionally graded aluminium/zirconia metal matrix composite synthesized by centrifugal casting' *Int. J. Mater. Res.*, vol. 106, no. 11, pp. 1174-1181, 2015.